RAPID COMMUNICATIONS

PHYSICAL REVIEW B VOLUME 47, NUMBER 5 1 FEBRUARY 1993-I

Two- and three-dimensional flux unbinding in $YBa_2Cu_3O_7$ thin films at small magnetic fields

S. Q. Chen, W. J. Skocpol, and E. DeObaldia
Department of Physics, Boston University, 590 Commonwealth Avenue, Boston, Massachusetts 02215

M. O'Malley
AT&T Bell Laboratories, Holmdel, New Jersey 07733

P. M. Mankiewich
Department of Physics, Boston University, 590 Commonwealth Avenue, Boston, Massachusetts 02215
and AT&T Bell Laboratories, Holmdel, New Jersey 07733
(Received 30 October 1992)

A vortex-unbinding mechanism for dissipation in epitaxial thin-film microstrips of $YBa_2Cu_3O_7$ is established for zero and small magnetic fields. Excellent self-consistent quantitative agreement is found with the two-dimensional Ginzburg-Landau Coulomb gas theory at low currents above the Kosterlitz-Thouless temperature T_k, and with a simple nucleation theory for three-dimensional vortex rings at higher currents and lower temperatures.

The cuprate high-temperature-superconducting materials are excellent examples of highly anisotropic, extreme type-II superconductors. Because the superconducting coherence length ξ is very small compared to the magnetic penetration depth λ, magnetic flux can enter the material in the form of current vortices. Dissipation results if the vortex core moves in the presence of a transport current. Vortex motion is limited by viscous drag, interactions with other vortices, and pinning to appropriate disorder in the material.

In this Rapid Communication, we investigate the behavior of thin films of $YBa_2Cu_3O_7$ (YBCO) near the transition temperature T_c in small or zero applied magnetic field. Zero applied field does not rule out the presence of vortices, if opposing vortices and antivortices are present in equal numbers.

At low currents, we find a temperature-dependent linear resistivity in excellent agreement with a two-dimensional (2D) theory of the unbinding of vortex-antivortex pairs by thermal fluctuations above a renormalized critical temperature T_k. In this regime the resistivity is set by flux flow dissipation and goes to zero below T_k. The transition width increases with decreasing sample quality [J_c(77 K)], and may be interpreted as an increase in the effective penetration depth.

At higher currents that probe a shorter length scale [see Eq. (3)], we find strongly nonlinear current-voltage characteristics with dissipation that persists to much lower temperatures. Our results here are consistent with the three-dimensional (3D) nucleation of small vortex rings that are expanded by the current. A simple model of the anisotropic self-interacting vortex ring accounts for the results, using the same penetration depths determined at low currents.

Our data is from thin films of YBCO produced by BaF_2-process coevaporation[1] onto room temperature $LaAlO_3$ substrates coated with a deep-UV patterned polymethyl-methacrylate (PMMA) resist stencil. After resist liftoff, appropriate postannealing converts the remaining material to fully oxygenated epitaxial YBCO.[2] Each pattern consisted of a long microstrip with current and voltage leads at each end divided into segments of lengths 1, 2, and 4 mm by additional voltage leads. Four-terminal zero-checking dc measurements resulted in an accuracy of $\sim 10^{-7}$ V. The thin-film substrate was mounted on a copper block immersed in temperature-controlled helium gas.

The zero-field resistive transition of a 2D superconducting thin film below the mean-field transition temperature T_{co} is expected to be dominated by the motion of free vortices of both polarities generated by the thermal unbinding of fluctuating vortex-antivortex pairs. Below a renormalized transition temperature T_k, binding is complete and no resistance is expected. The transition at T_k is usually referred to as the Kosterlitz-Thouless (KT) transition.[3,4] Because vortices interact logarithmically with distance, a connection can be established with the 2D Coulomb gas model.[5] Minnhagen has used numerical simulations[6] and data from extremely thin and uniform InOx films[7] to establish the "universal" behavior between T_k and T_{co} of the Ginzburg-Landau Coulomb gas (GLCG). This model predicts that the scaled resistivity ρ/ρ_N is a function only of $X = T(T_{co} - T_k)/T_k(T_{co} - T)$. This "GLCG scaling function"[8] is given by the solid curve in Fig. 1.

The data plotted in Fig. 1 is $\log(\rho)$ vs X measured at small fixed current densities ($j = 67,15,10$ A/cm^2 for Samples A, B, C, where length $= 7,2,3$ mm and width $= 30,100,30$ μm, respectively). These films differ in quality, as indicated by ρ_N(100 K) and J_c(77 K) (inset table). In all cases the resistivity is immeasurably small below $X = 1$ ($T < T_k$) and approaches a slowly varying resistivity for large X ($T \rightarrow T_{co}$). The parameters ρ_N, T_{co}, and T_k (lower box of inset table) were adjusted for best fit. The agreement is best for Sample A, our best film, which was strikingly homogeneous. (For Sample A,

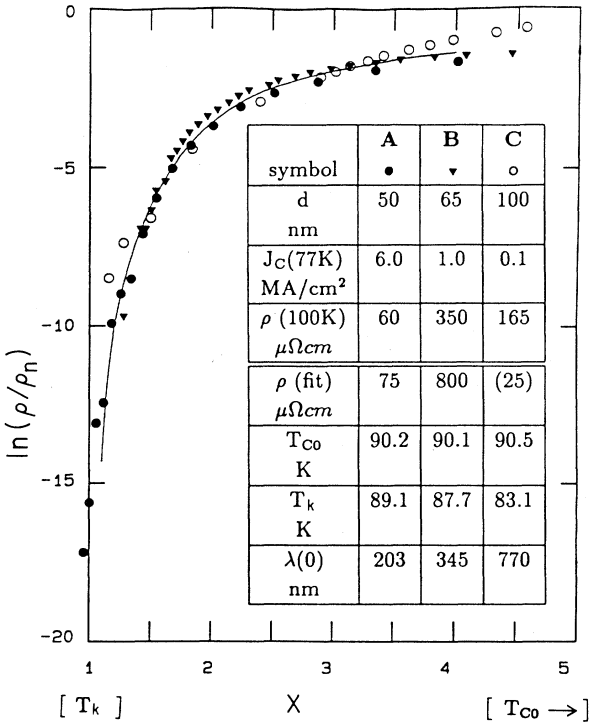

symbol	A ●	B ▼	C ○
d nm	50	65	100
Jc(77K) MA/cm²	6.0	1.0	0.1
ρ (100K) μΩcm	60	350	165
ρ (fit) μΩcm	75	800	(25)
Tco K	90.2	90.1	90.5
Tk K	89.1	87.7	83.1
λ(0) nm	203	345	770

FIG. 1. Universal scaling curve for resistivity vs scaled temperature for three samples of differing quality (inset table) compared to GLCG theory (solid curve).

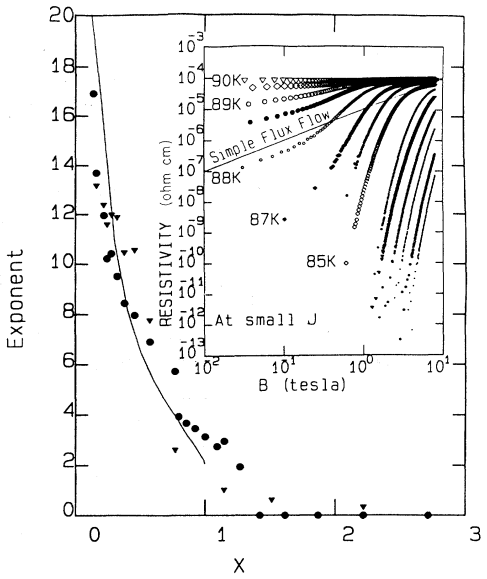

FIG. 2. Resistivity exponents $a-1$ (current, ●) and b (field, ▼) vs scaled temperature for Sample B, compared to GLCG theory (solid curve). The inset shows resistivity vs field characteristics from which b is derived.

all logρ vs log$j$ curves, not shown, were completely consistent for the three different segments of the film over the entire range $B=0$–8 T and $T=65$–90 K.) Samples B and C show wider transitions (lower T_k) and less consistency between segments (only the best is shown). Spatial inhomogeneity affects Sample C, since the fitted ρ_N corresponds to a small fraction of the full resistance of the entire segment.

The 2D GLCG model makes further scaling predictions.[5] In particular, the exponents $a-1$ and b (plotted in Fig. 2 with data from Sample B in solid dots and triangles) of the power-law behavior of the resistivity with respect to current density j and magnetic field B, respectively, are predicted to be a common function of X below $X=1$ ($T<T_k$), dropping suddenly to zero above T_k. The solid curve in Fig. 2 is the explicit prediction of the model, based on Fig. 26 and Eq. (4.63c) of Ref. 5. The jump from 2 to 0 at $X=1$ is the Nelson-Kosterlitz[4] "universal jump."

The inset of Fig. 2 shows an appropriate set of curves from Sample B for investigating the exponent b (the slope on this log-log plot). The main figure (triangles) shows that b vs X follows the expected magnitude and trend, but the slopes clearly remain nonzero above T_k ($=87.7$ K). This is probably because we have not investigated small enough values of B. The essential physics of the predicted zero slope is that above T_k the thermally unbound vortices of both polarities overwhelm the net difference between polarities associated with small applied B. A slope of 1 corresponds to simple flux flow with vortices of only one polarity. Larger values of B (and b) bring interactions between vortices into play.

The corresponding set of curves for Sample B with respect to current density j is shown in Fig. 3. The exponent $a-1$ derived from the slope at smallest measured log$j$ more clearly shows a jump from 0 to 2 near T_k. We have used the fitted T_k from Fig. 1 to determine X for

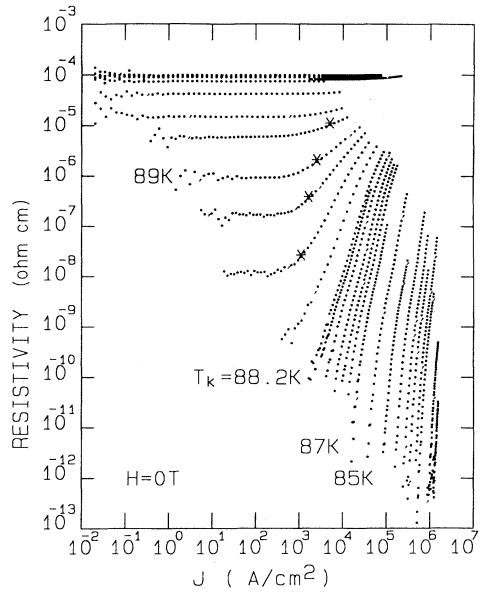

FIG. 3. Zero-field resistivity vs current density at various temperatures for Sample B. Asterisks mark the crossover to nonlinear behavior above J_k. The specific temperatures are 75 K, 77 K, 80–87 K (increment 1 K), 87–89 K (increment 0.2 K), and 89–92 K (increment 0.5 K).

Fig. 2. The slight discrepancy between the observed jump and this value of T_k may be because the rapidly plummeting region of flat resistivity moves below our measurement resolution. In this case the true jump is not observed.

Figure 2 shows that the exponents $a-1$ and b are quite consistent with each other and with the GLCG prediction. Despite this excellent agreement, we are not fully satisfied. Both the inset of Figs. 2 and 3 show a more complex behavior than simple power laws, and it is clear that there is a relationship between the B or j behavior below T_k and the nonlinearity (departures from simple power laws) above T_k. In Fig. 3 we have marked by an X the current J_X at which the nonlinearity has resulted in twice the resistivity that would be expected from the constant value at low j. We find that J_X is exponential in $T-T_k$ over the range 10^3–10^4 A/cm^2 extrapolating to about 10^2 A/cm^2 at T_k. (Note that the latter value depends sensitively on the choice of T_k.) A small field (0.1 T) preserves the slope but lowers T_k by about 1 K (or changes the prefactor accordingly).

We are unaware of a quantitative theory applicable to 2D systems of this thermally nucleated vortex unbinding in the presence of a transport current. Qualitatively, below T_k the dissipation comes from vortex-antivortex pairs ripped apart by the oppositely directed Lorentz forces resulting from the transport current. Larger currents unbind more tightly bound vortex pairs and hence probe shorter length scales. Above T_k the current-induced unbinding becomes significant only when it produces a density of vortices comparable to the thermally generated number.

The applicability of a 2D GLCG model to YBCO thin films 50–100 nm thick may seem surprising. Minnhagen and co-workers have argued that numerical studies of the anisotropic 3D X-Y model show a crossover to 2D behavior above a renormalized transition temperature T_k.[9] The GLCG model predicts a direct connection between the transition width $T_{co}-T_k$ and the thickness and penetration depth of the films.[10] With the help of Eq. (2) of Ref. 10 and the assumption $n^{2D}=n^{3D}d$, we get

$$\frac{T_k T_{co}}{T_{co}-T_k}=\frac{1}{8\times 1.65 k_B}\left[\frac{\Phi_0}{2\pi}\right]^2\frac{d}{\lambda^2(0)} .$$

If we use the actual thickness d of our films, the observed transition widths correspond to the $\lambda(0)$'s in Fig. 1 inset. Throughout this Rapid Communication we express the penetration depth λ in a two-fluid approximation

$$\lambda(T)=\lambda(0)\frac{2}{[1-(T/T_c)^4]^{1/2}} ,$$

where the factor of 2 normalizes the two-fluid function to agree near T_c with the linear dependence used above. The reduced J_c of Samples B and C can very plausibly be associated with a longer penetration depth[11] (less effective screening by supercurrents).

Because larger currents probe shorter length scales, we expect a dimensionality change when the scale probed is less than the film thickness. In an anisotropic 3D sample, vortex unbinding takes the form of the nucleation of ellipsoidal vortex rings with aspect ratio $\gamma>1$ that are further expanded by the transport current.[12] In the remainder of this Rapid Communication we compare our large-j data to this model, incorporating self-interaction effects since the critical ring radius is less than the penetration depth.

Following Ref. 12, but taking into account the anisotropy, the ring energy is

$$E_{\rm ring}=2\pi R\varepsilon_1-\frac{\pi J\Phi_0 R^2\gamma}{c} , \quad (1)$$

where R is the short radius in the c direction and the energy per unit length of interacting vortex ε_1 is

$$\varepsilon_1=\alpha_1\left[\ln\kappa+\ln\frac{2R}{\lambda}\right] . \quad (2)$$

Here $\alpha_1=(\Phi_0/4\pi\lambda)^2$, $\Phi_0=hc/2e$, $\kappa=\lambda/\xi\approx 100$, $\gamma=7.7$.[13,14] We have included a logarithmic term that accounts for the interaction between opposite sides of the ring since $\lambda\gg R$.

Because the length and energy per unit length anisotropies cancel, the first term is independent of γ. In the range of our interest, we find the critical radius:

$$R_c=4.0904\frac{\alpha_1 c}{J\Phi_0\gamma}-1.422\frac{\lambda}{\kappa} , \quad (3)$$

and barrier $Ba=E_{\rm ring}(R=R_c)$. If we let $\rho=\rho_{00}\exp(-Ba/k_BT)$ then,

$$\ln\frac{\rho}{\rho_{00}}=-\frac{Ba}{k_BT}=-\frac{J_T}{J}+\ln\rho_0+J\frac{2.025\pi\Phi_0\gamma\lambda}{\kappa^2 c k_B T} , \quad (4)$$

where

$$J_T=8.5506\frac{\pi c\alpha_1^2}{\Phi_0\gamma k_B T}=\frac{(1-t^4)^2}{t}J_T(0) , \quad (5)$$

TABLE I. Characteristic currents (A/cm^2).

		A	B	C
$J_T(0)$	Measured	5.6×10^8	9.0×10^7	1.3×10^7
$J_T(0)$	Calculated	3.7×10^8	4.5×10^7	1.9×10^7
J_c(77 K)	Measured	6.0×10^6	1.0×10^6	1×10^5
J_d (77 K)	Calculated	3.2×10^5	7.4×10^4	6.3×10^3
J_c (85 K)	Measured	5.8×10^5	1.3×10^5	
J_d (85 K)	Calculated	1.1×10^5	1.8×10^4	

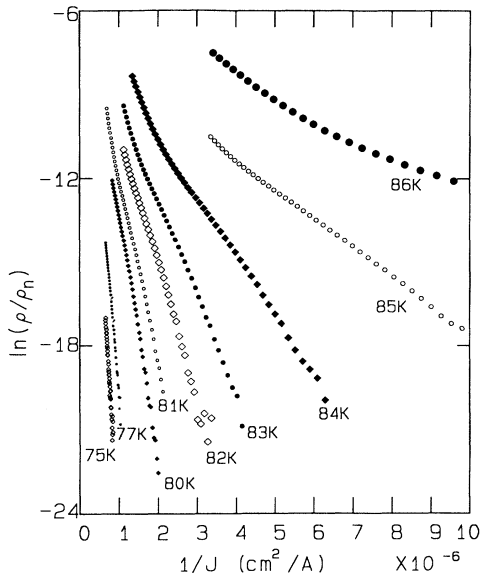

FIG. 4. Natural logarithm of normalized resistivity vs inverse current density at various temperatures for Sample B.

and

$$\ln\rho_0 = 8.791\frac{\pi\alpha_1\lambda}{\kappa k_B T} = \frac{(1-t^4)^{1/2}}{t}\rho(0)+\ln\rho_{00}\ , \qquad (6)$$

and $t = T/T_k$. We expect dimensional crossover to 3D above a current J_d such that $R_c(J_d) = d$, giving

$$J_d = \frac{4.09c\Phi_0}{4^2\pi^2\lambda^2\gamma(1.422\lambda/\kappa + d)}\ . \qquad (7)$$

The 3D model predicts that $\ln\rho$ is linear in $1/J$, with slope J_T and intercept $\ln\rho_0$ except for a negligible term proportional to J. Figure 4 shows the data from Sample B plotted in this way. Except for deviations at higher resistances [$\ln(R/R_n) > -12$], a linear fit is appropriate. The slopes J_T at different temperatures yield a straight line when plotted against the predicted temperature dependence Eq. (5). The measured and calculated values of $J_T(0)$ for all three samples are given in Table I. Excellent agreement is obtained. The calculated values are based on the penetration depth parameter from Fig. 1 inset. As an important self-consistency check, we calculate that J_d is always substantially smaller than J_c, so that a 3D analysis is justified.

TABLE II. Analysis of prefactors.

		A	B	C
$\rho(0)$	Measured	13.5	9.06	2.7
$\rho(0)$	Calculated	146	87.2	41.5
$\ln\rho_{00}$	Measured	−15.3	−17.1	−15.2

Our 3D model also successfully predicts the temperature dependence of the prefactor, Eq. (6), but not its coefficient. (See Table II.) This term arises from our presumably inadequate treatment of the self-interaction across the vortex ring.

In summary we have found that vortex unbinding in two and three dimensions accounts quantitatively for most aspects of the zero-field resistive transition of YBCO thin films.

We gratefully acknowledge helpful conversations with Petter Minnhagen. This work was supported by DARPA (MDA972-88-K-005) through a subcontract from the University of California at Santa Barbara, by DARPA/ONR (N00014-90-J-4033), and by the Consortium for Superconducting Electronics (DARPA MDA972-90-C-0021).

[1]P. M. Mankiewich *et al.*, Appl. Phys. Lett. **51**, 1753 (1987).
[2]P. M. Mankiewich *et al.*, Mat. Res. Soc. Symp. Proc. **99**, 119 (1988).
[3]J. M. Kosterlitz and D. J. Thouless, J. Phys. C **6**, 1181 (1973).
[4]David R. Nelson and J. M. Kosterlitz, Phys. Rev. Lett. **39**, 1201 (1977).
[5]Petter Minnhagen, Rev. Mod. Phys. **59**, 1001 (1987).
[6]H. Weber and P. Minnhagen, Phys. Rev. B **38**, 8730 (1988).
[7]A. F. Hebard and A. T. Fiory, Phys. Rev. Lett. **50**, 1603 (1983).
[8]Petter Minnhagen and Peter Olsson (unpublished).
[9]Petter Minnhagen and Peter Olsson, Phys. Rev. Lett. **67**, 1039 (1991).
[10]Petter Minnhagen and Peter Olsson, Phys. Rev. B **45**, 5722 (1992).
[11]A. T. Fiory, A. F. Hebard, P. M. Mankiewich, and R. E. Howard, Phys. Rev. Lett. **61**, 1419 (1988).
[12]Daniel S. Fisher, Matthew P. A. Fisher, and David A. Huse, Phys. Rev. B **43**, 130 (1991), Sec. III.
[13]D. E. Farrell (unpublished).
[14]G. J. Dolan *et al.*, Phys. Rev. Lett. **62**, 2184 (1989).